

A glassy carbon electrode modified with a composite consisting of reduced graphene oxide, zinc oxide and silver nanoparticles in a chitosan matrix for studying the direct electron transfer of glucose oxidase and for enzymatic sensing of glucose

Zhenjiang Li^{1,2} · Liying Sheng¹ · Alan Meng² · Cuicui Xie¹ · Kun Zhao²

Received: 12 November 2015 / Accepted: 10 February 2016 / Published online: 29 February 2016
© Springer-Verlag Wien 2016

Abstract The authors describe the fabrication of a nanocomposite consisting of reduced graphene oxide, zinc oxide and silver nanoparticles by microwave-assisted synthesis. The composite was further reduced in-situ with hydrazine hydrate and then placed, along with the enzyme glucose oxidase, on a glassy carbon electrode. The synergistic effect of the materials employed in the nanocomposite result in excellent electrocatalytic activity. The Michaelis-Menten constant of the adsorbed GOx is 0.25 mM, implying a remarkable affinity of the GOx for glucose. The amperometric response of the modified GCE is linearly proportional to the concentration of glucose in 0.1 to 12.0 mM concentration range, and the detection limit is 10.6 μ M. The biosensor is highly selective, well reproducible and stable.

Keywords Biosensor · Bioassay · Enzymatic assay · Nanocomposite Microwave synthesis · In-situ reduction · Hydrazine reduction · Direct electrochemistry · Amperometry

Introduction

Biosensors based on the direct electrochemistry of redox enzymes/proteins have been investigated extensively up to now [1, 2]. These biosensors not only can avoid expensive or harmful mediators, but also have high selectivity and sensitivity. Furthermore, the mechanism of electron transfer for direct electrochemistry of redox enzymes/proteins is intensive studied [3, 4]. In the field of monitoring the glucose levels in serum or urine, glucose biosensors based on the direct electrochemistry of GOx are mainly used [5]. However, the direct electron transfer (DET) between the GOx and electrodes is usually hindered because the redox-active flavin adenine dinucleotide (FAD) cofactors of GOx are deeply buried within the insulated prosthetic shells [6]. Intensive efforts have been devoted to retaining the biological activity and promoting the direct electron transfer behaviors of GOx by selecting suitable matrix [7, 8].

The development of nanotechnology offers new horizons for the application of nanomaterials in bioelectrochemical analysis [7, 8]. Graphene is a two-dimensional nanosheet composed of hexagonal arrayed sp^2 hybridized carbon atoms with one-atomic thickness [9]. Due to the unique structure, it possesses numerous excellent properties such as fast electron transportation, a high specific surface area, and good biocompatibility, which result in promising applications in electrochemical sensors [10]. It has been reported that graphene modified electrode can be successfully applied to detect glucose [11, 12].

Electronic supplementary material The online version of this article (doi:10.1007/s00604-016-1791-x) contains supplementary material, which is available to authorized users.

✉ Alan Meng
alanmengqust@163.com

¹ Key Laboratory of Polymer Material Advanced Manufacturing Technology of Shandong Provincial, College of Electromechanical Engineering, College of Sino-German Science and Technology, Qingdao University of Science and Technology, Qingdao 266061, Shandong, People's Republic of China

² State Key Laboratory Base of Eco-chemical Engineering, College of Chemistry and Molecular Engineering, Qingdao University of Science and Technology, Qingdao 266042, Shandong, People's Republic of China

In addition, nanostructured metal oxides are known to have unique ability to promote faster electron transfer kinetics between electrode and the active site of desired enzyme [8]. Among the metal oxide, ZnO have been exploited as a potential material for biosensing, due to its strong adsorption ability (high isoelectric point ~ 9.5) [13], which is more favorable for the immobilization of various redox active enzymes, such as tyrosinase, uricase etc. [14, 15]. Compared to ZnO, doping noble metals in ZnO [16, 17] offers an effective approach to enhance the electrocatalytic activity of ZnO nanostructures, which is crucial for their practical applications especially for the construction of biosensor. The metal-ZnO nanostructures built a favorable bridge for electron transportation between the electrode and the detecting substrate.

The glucose biosensors based on GR [12], GR-ZnO [18], ZnO [19], Ag-ZnO nanocomposites [20] have been reported, but there are some problems in the above mentioned biosensors, for example, some have the narrow detection range, some have high detection limit, some have unsatisfactory stability, etc. To the best of our knowledge, no studies have been reported about using Ag nanoparticles with rGO-ZnO nanostructures as an electrode material for glucose biosensors.

In the present work, the rGO_(HHA)-ZnO-Ag nanocomposites are acquired by microwave-assisted method and then reduced in situ by using 85 % hydrazine hydrate. The nanocomposites can provide a favorable microenvironment for GOx to realize direct electrochemistry. The synergistic effect of rGO_(HHA), ZnO, Ag result in excellent electrocatalytic activity. The rGO_(HHA)-ZnO-Ag modified electrode displays a series of excellent features such as wide linearity, low detection limit and low Michaelis-Menten constant (k_m^{app}). The selectivity, reproducibility, stability of rGO_(HHA)-ZnO-Ag modified electrode has also been studied in detail. It is a worthwhile exploration for fabricating other biosensor by using multi-components electrode materials.

Experimental

Reagents

GOx ($>100 \text{ u}\cdot\text{mg}^{-1}$), glucose (MW: 198.17), chitosan (CS), dopamine (DA, $>98 \%$, MW: 189.64), L-ascorbic acid (AA, $>99 \%$, MW: 176.12) and uric acid (UA, $>99 \%$, MW: 168.11) were purchased from Sangon-Biotech Co., Ltd. (<http://www.sangon.com/>). Graphite powder, zinc acetate dihydrate ($\text{Zn}(\text{CH}_3\text{COO})_2\cdot 2\text{H}_2\text{O}$), silver nitrate (AgNO_3) and hydrazine hydrate (85 %) were purchased from Sinopharm Chemical Reagent Co., Ltd. (<http://www.sinoreagent.com.cn>). Phosphate buffers were prepared by mixing the solutions of 0.2 M KH_2PO_4 and 0.2 M Na_2HPO_4 . Other chemicals were of analytical-reagent grade without further purification. All the solutions were prepared using double distilled water.

Apparatus

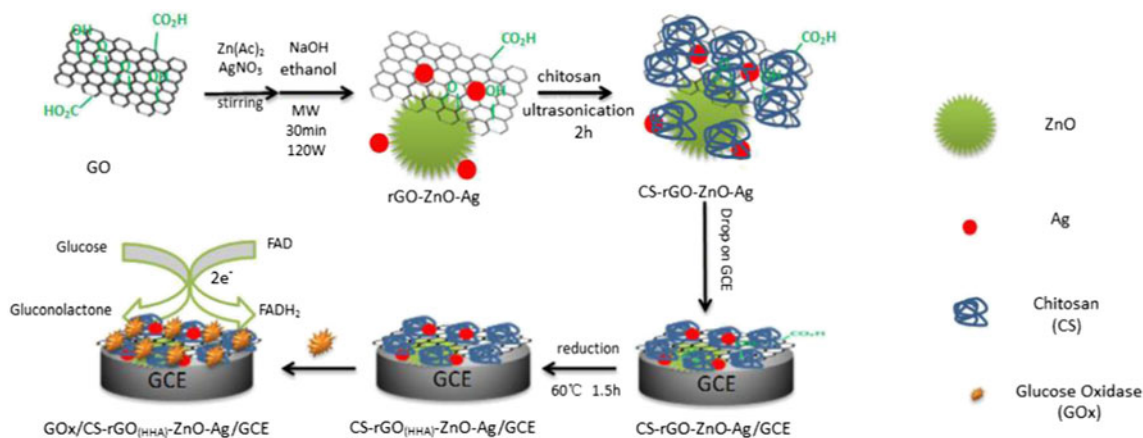
All electrochemical experiments were carried out on a CHI660E electrochemistry workstation (Shanghai CH Instrument Company, China). A three-electrode system was used with a saturated calomel electrode (SCE) as the reference electrode, a modified glassy carbon electrode (GCE) as the working electrode and a platinum wire as the counter electrode. The structure and morphology of rGO-ZnO-Ag were characterized by a D8ADVANCE X-ray diffractometer, a Renishaw InVia laser micro Raman spectrometer, a JSM-6700F scanning electron microscope and a JEM-200Ex transmission electron microscope, respectively.

Preparation of CS-rGO-ZnO-Ag nanocomposites

Graphene oxide (GO) [21] and rGO-ZnO-Ag [22] nanocomposites were obtained by microwave-assisted method according to the previously reported by our group. The detailed preparation process of GO is given in the Electronic Supplementary Material (ESM). The preparation of rGO-ZnO-Ag includes the following steps: Firstly, under stirring, GO suspension was added into the mixed solution of Zn ($\text{CH}_3\text{CH}_2\text{COO}$)₂ and AgNO_3 . Then, NaOH solution and ethanol was added into the mixed solution. The mixture was then placed in a microwave reactor and treated for 30 min with a power of 120 W. Finally, the rGO-ZnO-Ag was acquired. CS solution was prepared by adding 10 mg CS flakes into 10 mL 1 % acetate buffer and stirred for 10 min. 10 mg of the synthesized rGO-ZnO-Ag powder was dispersed into CS solution by mild ultrasonication for 2 h to form homogeneous suspensions. Finally $1.0 \text{ mg}\cdot\text{mL}^{-1}$ of CS-rGO-ZnO-Ag suspension was prepared.

Fabrication of GOx/CS-rGO_(HHA)-ZnO-Ag/GCE electrodes

A bare glassy carbon electrode was polished to mirror-like with 0.3 and 0.05 μm alumina slurry, then sequentially sonicated in double distilled deionized water, anhydrous ethanol for 3 min. After the electrode was dried in nitrogen, 5 μL CS-rGO-ZnO-Ag ($1.0 \text{ mg}\cdot\text{mL}^{-1}$) suspension was dropped on the surface of the cleaned GCE and dried naturally in the air. The obtained electrode was noted as CS-rGO-ZnO-Ag/GCE. The CS-rGO-ZnO-Ag/GCE was immersed in 85 % hydrazine hydrate, and then heated at 60 °C for 1.5 h. After that, the electrode was rinsed with 0.1 M phosphate buffer and double distilled water, respectively. The obtained electrode was noted as CS-rGO_(HHA)-ZnO-Ag/GCE. 5 μL GOx ($6 \text{ mg}\cdot\text{mL}^{-1}$) solution was spread onto the surface of the CS-rGO_(HHA)-ZnO-Ag/GCE electrode and then the electrode was left inside a refrigerator (4 °C) overnight. The prepared GOx/CS-rGO_(HHA)-ZnO-Ag/GCE was stored at 4 °C when not in use. The whole process



Scheme 1 Schematic illustration of CS-rGO_(HHA)-ZnO-Ag composites modified GCE electrode

of biosensor preparation is outlined in Scheme 1. For comparison, GO_x/GCE, CS-rGO_(HHA)-ZnO/GCE, GO_x/CS-rGO_(HHA)-ZnO/GCE, CS-rGO_(HHA)-ZnO-Ag/GCE were prepared using a similar procedure. All of the modified electrodes were stored at 4 °C in refrigerator when not in use.

Electrochemical measurement

All experiments were carried out at the ambient temperature in 0.1 M phosphate buffer as the supporting electrolyte. The cyclic voltammetric measurements were recorded from −0.1 to 0.8 V at a scan rate of 100 mV·s^{−1}. The differential pulse voltammetry measurements for glucose detection were performed from −0.2

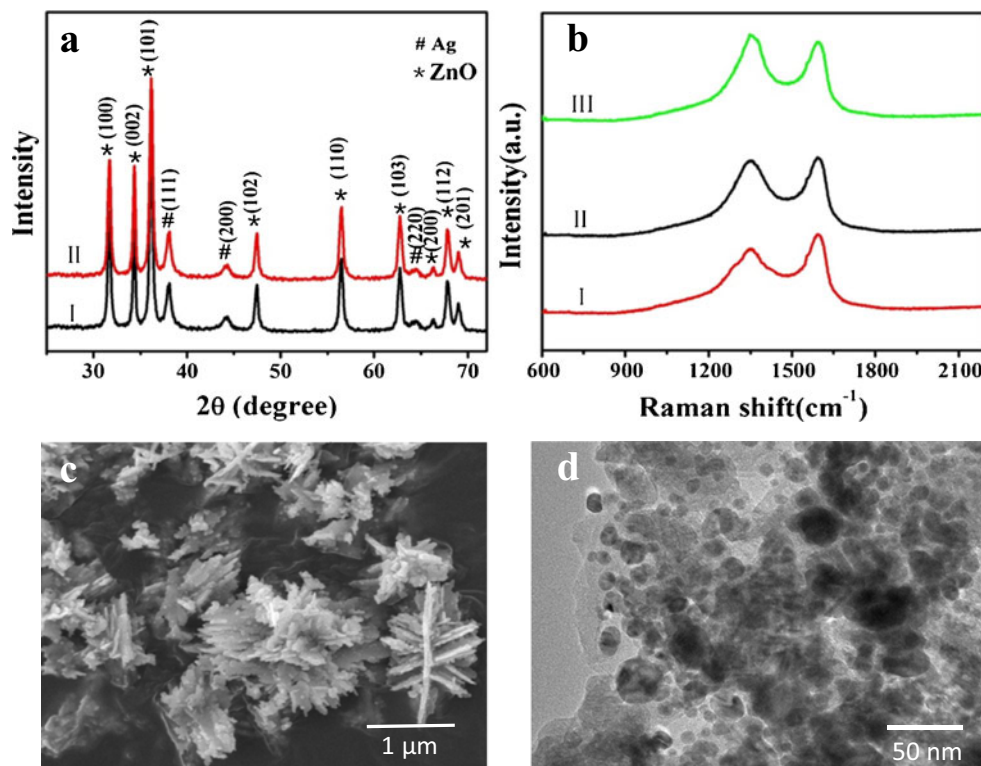
to −0.8 V with a pulse amplitude of 50 mV and width of 50 ms in the air-saturated solutions.

Results and discussion

Characterization

Figure 1a shows the XRD spectra of rGO-ZnO-Ag composites (I) and rGO_(HHA)-ZnO-Ag composites (II). The characteristic diffraction peaks at 2θ of 31.7°, 34.4°, 36.3°, 47.4°, 56.5°, 62.7°, 66.2°, 67.8° and 68.9° are assigned to (100), (002), (101), (102), (110), (103), (200), (112) and (201) plane

Fig. 1 **a** XRD spectra of rGO-ZnO-Ag (I) and rGO_(HHA)-ZnO-Ag composites (II), **b** The Raman spectra of GO (I) rGO-ZnO-Ag (II) and rGO_(HHA)-ZnO-Ag composites (III), **c** SEM images of rGO-ZnO-Ag composites, **d** TEM images of rGO-ZnO-Ag composites



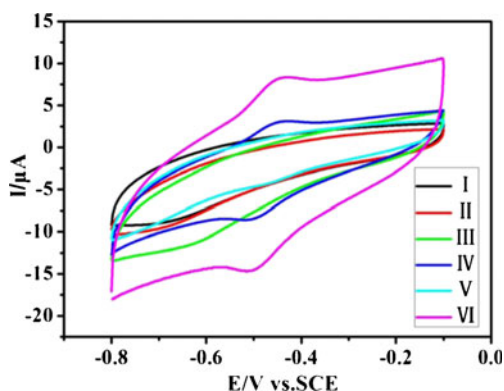


Fig. 2 The cyclic voltammograms of GCE (I), GOx/GCE (II), CS-rGO_(HHA)-ZnO/GCE (III), GOx/CS-rGO_(HHA)-ZnO/GCE (IV), CS-rGO_(HHA)-ZnO-Ag/GCE (V) and GOx/CS-rGO_(HHA)-ZnO-Ag/GCE (VI) in phosphate buffer (0.1 M, pH 7.4) at the scan rate of 100 mV·s⁻¹

of ZnO with a hexagonal (wurtzite) ZnO phase (JCPDS 36-1451). The three small peaks at 2θ of 38.1°, 44.3° and 64.4° correspond to (111), (200) and (220) planes of face-centered-cubic (FCC) metallic Ag (JCPDS 04-0783). The diffraction peaks for rGO are not observed, which may be related to the low amount and low diffraction intensity. ZnO and Ag nanoparticles coexist whether it reduced by hydrazine hydrate or not.

Figure 1b shows the Raman spectra of GO (I), rGO-ZnO-Ag (II) and rGO_(HHA)-ZnO-Ag(III). It is well known that GO exhibits two characteristic peaks of D band at 1350 cm⁻¹ and G band at 1594 cm⁻¹. The G band is attributed to the in-plane vibration of sp² bonded carbon atoms while the D band suggests the presence of defects within the hexagonal graphite structure [23]. It was found that the intensity ratio of the D to G band (I_D/I_G) increased from 0.8583 of GO to (0.9835 ± 0.0139) of rGO composite, which indicated GO was partly reduction in microwave reaction. As shown in Fig. 1b (III), the I_D/I_G increased to 1.0249 which indicates that the rGO in the composites is further deoxidized by 85 % hydrazine hydrate. Therefore, it can be inferred that the conductivity is improved.

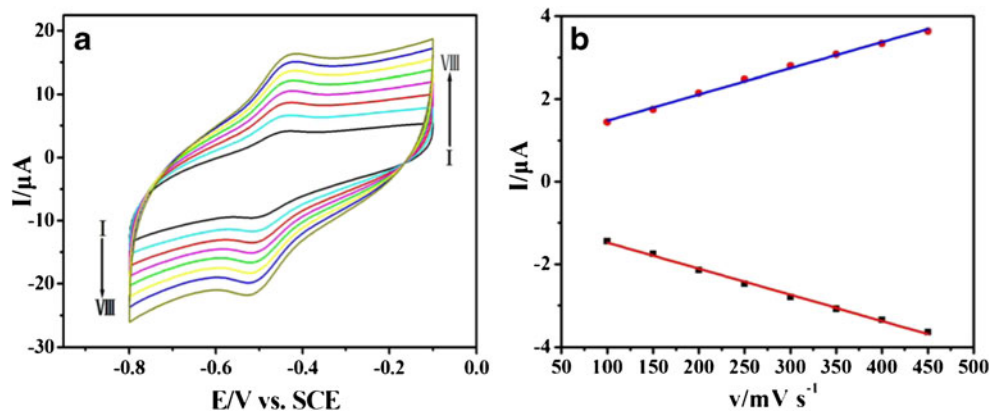
Figure 1c shows the SEM images of rGO-ZnO-Ag nanocomposites. As can be seen from SEM, the flower-like ZnO

microstructures are assembled by many interleaving nanosheets which have the uniform thickness. The surfaces of ZnO sheets are not very smooth, there are some particles and pits on the surface of ZnO sheets, the particles may be Ag nanoparticles. Figure 1d shows the TEM images of rGO-ZnO-Ag nanocomposites. We can find that rGO sheets, ZnO sheets and Ag nanoparticles all exist in rGO-ZnO-Ag nanocomposites. Ag nanoparticles are distributed on the whole ZnO nanosheets. Obviously, the rGO sheets and Ag nanoparticles are attached on the surface of ZnO nanosheets, which confirms the perfect preparation of these ternary composites.

Evaluation of the electrochemical performance of modified electrode

To inspect the direct electrochemical behavior of GOx adsorbed on the CS-rGO_(HHA)-ZnO-Ag/GCE, the cyclic voltammograms of GCE, GOx/GCE, CS-rGO_(HHA)-ZnO/GCE, GOx/CS-rGO_(HHA)-ZnO/GCE, CS-rGO_(HHA)-ZnO-Ag/GCE and GOx/CS-rGO_(HHA)-ZnO-Ag/GCE electrodes in phosphate buffer(0.1 M, pH 7.4) at the scan rate of 100 mV·s⁻¹ are displayed in Fig. 2. The bare GCE (Curve I), CS-rGO_(HHA)-ZnO/GCE (Curve III) and CS-rGO_(HHA)-ZnO-Ag/GCE (Curve V) with no GOx do not show any electrochemical features in the cyclic voltammograms, indicating that there is no redox reactions on the electrodes in the investigated potential range. The GOx/GCE (Curve II) still shows no electrochemical signal owing to the poor immobilization of GOx on the GCE surface. However, a pair of redox peaks occurs in the cyclic voltammogram (Curve IV) of GOx/CS-rGO_(HHA)-ZnO/GCE which is ascribed to the facilitated redox reaction of FAD/FADH₂ couple in GOx on the electrode surface, although it is very weak. Remarkably, GOx/CS-rGO_(HHA)-ZnO-Ag/GCE exhibits a pair of stronger redox peaks as seen from Curve VI. It is suggested that Ag plays a synergy role in facilitating the electron transfer and CS-rGO_(HHA)-ZnO-Ag composites have assisted DET from the active site of GOx to electrodes. In the microenvironment of CS-rGO_(HHA)-

Fig. 3 a The cyclic voltammograms of GOx/CS-rGO_(HHA)-ZnO-Ag/GCE at various scan rates in phosphate buffer (0.1 M, pH 7.4), From curve I to VIII corresponding to 100, 150, 200, 250, 300, 350, 400, 450 mV·s⁻¹, b Relationship between scan rate and the cathodic and anodic peak currents



ZnO-Ag, GOx can easily react with electrode, which can eventually amplify the DET signal of GOx [24]. Moreover, it exhibits a well-defined wave around -0.513 V (vs. SCE) with 38.5 mV separation between the oxidation and reduction peaks at 100 $\text{mV}\cdot\text{s}^{-1}$, indicating that the prosthetic FAD groups of GOx still retain their bioactivity after the adsorption process [25]. Herein, the CS-rGO_(HHA)-ZnO-Ag nanocomposite can be very effective in facilitating the electron transfer between active sites of GOx and the underlying GCE.

Figure 3a shows cyclic voltammograms of the GOx/CS-rGO_(HHA)-ZnO-Ag/GCE electrode at scan rates of 100, 150, 200, 250, 300, 350, 400 and 450 $\text{mV}\cdot\text{s}^{-1}$. With the increase of the scan rate, both the anodic and cathodic peak currents increase linearly (Fig. 3b). These electrochemical characteristics indicate that the reaction is a surface-controlled process. At the same time, the ratio between the anodic and cathodic peak currents and E° (the formal potential) of the adsorbed GOx keep almost unchanged. This shows that the electron transfer between GOx and GCE can be easily performed in the presence of CS-rGO_(HHA)-ZnO-Ag composites and it is a typical quasi-reversible process [26]. According to the Laviron formula $k_s = mnFv/RT$ when $n\Delta E_p < 200$ mV [27], where m is a parameter related to the peak-to-peak separation, n is the number of electrons involved in the electrochemical process, F is the Faraday constant, v is the scan rate, R is the molar gas constant and T is the thermodynamic temperature, ΔE_p is the peak-to-peak separation, the average electron transfer rate constant (k_s) of GOx adsorbed on CS-rGO_(HHA)-ZnO-Ag/GCE is estimated to be about (2.85 ± 0.04) s^{-1} . This value is higher than those for GOx assemble on graphene (2.68 s^{-1}) [28] and GOx on poly (methylene blue) doped silica nanocomposites (2.44 s^{-1}) [29]. This implies that the CS-rGO_(HHA)-ZnO-Ag nanocomposites can facilitate to the electron transfer between GOx and electrode.

The effect of different pH at GOx immobilized CS-rGO_(HHA)-ZnO-Ag nanocomposites modified electrode is investigated. As seen from the Fig. 4a, both the anodic and the cathodic peak potentials shifted negatively with the increase

Fig. 4 a pH values study of GOx/CS-rGO_(HHA)-ZnO-Ag/GCE electrode in phosphate buffer (0.1 M, pH 7.4) at the scan rate of 100 $\text{mV}\cdot\text{s}^{-1}$, b Plot of E° vs. pH values

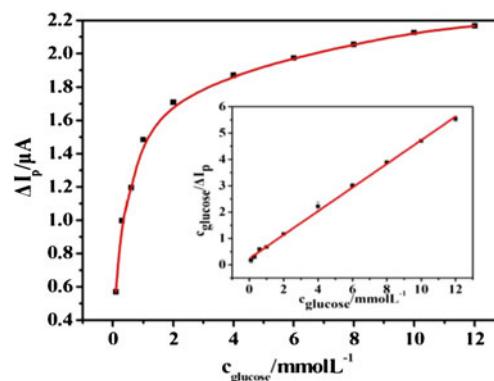
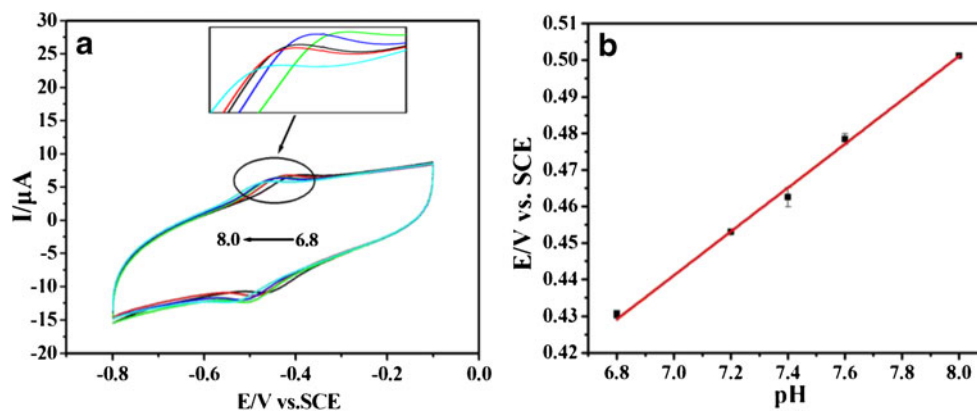


Fig. 5 The peak current change vs. glucose concentration. Insert: peak current change vs. glucose concentration

of pH from 6.8 to 8.0. It means that the H^+ exchange participated in the electrochemical reaction of GOx [30]. The maximum current response occurred at pH 7.4. Consequently, phosphate buffer of pH 7.4 was employed in the subsequent glucose detection. The relationship between the E° and pH value is shown in Fig. 4b. The plots exhibits a linear relationship with a slope of -59.4 $\text{mV}\cdot\text{pH}^{-1}$, being close to the expected value of -59 $\text{mV}\cdot\text{pH}^{-1}$. It indicates that two protons participate in the electron transfer process.

Electrochemical detection of glucose at the GOx/CS-rGO_(HHA)-ZnO-Ag/GCE

Figure 5 shows a plot of the peak current change (ΔI_p) before and after glucose introduction against the glucose concentration (c_{glucose}). The differential pulse voltammograms of GOx/CS-rGO_(HHA)-ZnO-Ag/GCE in air-saturated phosphate buffer (0.1 M, pH 7.4) with different glucose concentration is shown in Fig. S1. The peak current decreased when the glucose content was increased. Obviously, the ΔI_p value rises when the c_{glucose} value increased in Fig. 5. It can be found that these data were fitted well to an empirical saturating model. As shown in the inset of Fig. 5, the $c_{\text{glucose}}/\Delta I_p$ displays a linear response with respect to c_{glucose} over the range of glucose concentration

Table 1 Comparison of different modified electrodes for glucose determination

Electrode	k_m^{app}	Linear range	Detection limit	Reference
GOx/TiO ₂ -graphene/GCE	-	0.0–8.0 mM	-	[32]
Graphene-CdS-GOD/GCE	1.6 mM	2.0–16 mM	70 μ M	[33]
AuNPs/GOD-MWCNTs-PVA/GCE	-	0.5–8.0 mM	20 μ M	[34]
GOx/Au-chitosan/GCE	3.5 mM	0.05–1.3 mM	13 μ M	[35]
GOx/CS-rGO _(HHA) -ZnO-Ag/GCE	0.25 mM	0.1–12.0 mM	10.6 μ M	This work

from 0.1 to 12.0 mM. The regression equation was $c_{\text{glucose}}/\Delta I_p = 0.4485c_{\text{glucose}} + 0.2519$ with a high correlation coefficient of 0.999 and the detection limit (at signal-to-noise of 3) was estimated as 10.6 μ M. The apparent Michaelis-Menten constant (k_m^{app}) which indicates the enzyme-substrate kinetics can be used to estimate the biological activity of the immobilized enzyme. According to the Lineweaver-Burke equation, $1/v = 1/V_{\text{max}} + k_m^{app}/(V_{\text{max}}[S])$ [31], where v is the reaction rate after the addition of glucose, S is the bulk concentration of the substrate, and V_{max} is the maximum reaction rate of enzyme, the corresponding plot yielded an apparent k_m^{app} value of 0.25 mM, which was much lower than the glucose biosensors reported in the literature (Table 1). The small k_m^{app} value indicates that the immobilized enzymes possess high enzymatic activity.

Table 1 gives the comparison of analytical parameters of the reported biosensors, including the Michaelis-Menten constant, the linear range and the detection limit. It is found that the GOx/CS-rGO_(HHA)-ZnO-Ag/GCE biosensor exhibited satisfactory detection limit and Michaelis-Menten constant. The reasons might be attributed to the synergistic effect of rGO_(HHA), ZnO, Ag result in excellent electrocatalytic activity, which can enhance the access chance of the GOx and glucose.

The selectivity, reproducibility and stability of the biosensor

We examined the selectivity of the GOx/CS-rGO_(HHA)-ZnO-Ag/GCE by measurement of several common electroactive contaminants in blood: dopamine (DA), ascorbic acid (AA) and uric acid (UA). As shown in Fig. S2, the changes of peak

current caused by 1.0 mM dopamine, 1.0 mM ascorbic acid and 1.0 mM uric acid accounted for 9.69 %, 5.63 % and 5.42 % of that derived from 0.5 mM glucose, respectively, in phosphate buffer (pH 7.4). It proves that the developed biosensor had an acceptable selectivity.

Under the optimized pH = 7.4 conditions, 0.5 mM glucose in air-saturated phosphate buffer was measured by the same modified electrode for 5 times. The relative standard deviation (RSD) of the peak current was only 4.6 %, which demonstrates that the biosensor has a good reproducibility. Furthermore, 0.5 mM glucose in air-saturated phosphate buffer was measured by five modified electrodes. The RSD of the peak current was 6.7 %, revealing an acceptable repeatability. Additional experiments were carried out to test the stability. After the electrode was stored for 7 days at 4 °C in fridge, it still retain 89.6 % of its original response, which suggests that GOx/CS-rGO_(HHA)-ZnO-Ag/GCE electrode has good storage stability.

Detection of glucose in blood serum samples

In order to illustrate the practical usage of this biosensor, it was applied to detect glucose in blood serum samples with no pretreatment. All of the concentrations of glucose determined are in the linear response range. As can be seen from Table 2, the results are satisfactory and in accordance with those measured by the biochemical analyzer in the hospital. The recovery rates of the glucose solution added to blood serum samples were from 93.6 to 102.5 %. These results indicated the reliability of this biosensor for glucose determination in real samples. This sensor was used to detect the glucose in the

Table 2 Determination of glucose in blood serum samples

Serum sample	biochemical analyzer value (mM)	Determined value ^a (mM)	RSD (%)	Relative Deviation (%)	Glucose added (mM)	Glucose found ^a (mM)	Recovery (%)
1	4.31	4.12 ± 0.12	2.78	-4.41	1.0	0.981 ± 0.0032	98.1
2	4.68	4.83 ± 0.19	4.06	3.21	1.0	0.936 ± 0.0070	93.6
3	3.72	3.56 ± 0.19	5.11	-4.30	1.0	0.989 ± 0.0056	98.9
4	3.06	3.27 ± 0.08	2.61	6.86	1.0	1.025 ± 0.0061	102.5

^a Average value from three determinations

serum samples without dilution, which can be more accurate to reflect the real situation in the serum samples.

Conclusions

In summary, a biosensor for monitoring glucose was fabricated by immobilization GOx on rGO_(HHA)-ZnO-Ag modified glassy carbon electrode. The rGO_(HHA)-ZnO-Ag nanocomposites offered a favorable microenvironment for the direct electrochemistry of GOx. The adsorbed GOx displays a pair of well-defined quasi-reversible redox peaks at a potential of -0.513 V (vs. SCE). Due to the synergistic effects of rGO_(HHA), ZnO and Ag, the GOx/CS-rGO_(HHA)-ZnO-Ag/GCE showed a broad linear measuring range (0.1–12 mM), low detection limit (10.6 μ M) and low Michaelis-Menten constant (0.25 mM). Moreover, it also had acceptable reproducibility, stability, selectivity and determined glucose in human serum with satisfactory result. Maybe it is a worthwhile exploration for fabricating other biosensor by using multi-components electrode materials.

Acknowledgments The work reported here was supported by the National Natural Science Foundation of China under Grant No.51572137, 51502149, 51272117, 51172115, the Natural Science Foundation of Shandong Province under Grant No.ZR2015PE003, ZR2013EMQ006, the Research Award Fund for Outstanding Young Scientists of Shandong Province Grant No. BS2013CL040, the Specialized Research Fund for the Doctoral Program of Higher Education of China under Grant No. 20123719110003, the Tackling Key Program of Science and Technology in Shandong Province under Grant No. 2012GGX1021, the Application Foundation Research Program of Qingdao under Grant No. 13-1-4-117-jch, 15-9-1-28-jch, 14-2-4-29-jch, Shandong Province Taishan Scholar Project. We express our grateful thanks to them for their financial support.

Compliance with ethical standards must be captured The author(s) declare that they have no competing interests

References

- Karyakin AA (2012) Principles of direct (mediator free) bioelectrocatalysis. *Bioelectrochemistry* 88:70–75
- Habermüller K, Mosbach M, Schuhmann W (2000) Electron-transfer mechanisms in amperometric biosensors. *Fresenius J Anal Chem* 366:560–568
- Gu M, Wang J, Tu Y, Di J (2010) Fabrication of reagentless glucose biosensors: a comparison of mono-enzyme GOD and bienzyme GOD-HRP systems. *Sensors Actuators B Chem* 148:486–491
- Deng CY, Chen JH, Nie Z, Si SH (2010) A sensitive and stable biosensor based on the direct electrochemistry of glucose oxidase assembled layer-by-layer at the multiwall carbon nanotube-modified electrode. *Biosens Bioelectron* 26:213–219
- Wilson R, Turner APF (1992) Glucose oxidase: an ideal enzyme. *Biosens Bioelectron* 7:165–185
- Holland JT, Lau C, Brozik S, Atanassov P, Banta S (2011) Engineering of glucose oxidase for direct electron transfer via site-specific gold nanoparticle conjugation. *J Am Chem Soc* 133:19262–19265
- Su S, Sun HF, Xu F, Yuwen LH, Fan CH, Wang LH (2014) Direct electrochemistry of glucose oxidase and a biosensor for glucose based on a glass carbon electrode modified with MoS₂ nanosheets decorated with gold nanoparticles. *Microchim Acta* 181:1497–1503
- Karupiah C, Palanisamy S, Chen SM, Veeramani V, Periakaruppan P (2014) Direct electrochemistry of glucose oxidase and sensing glucose using a screen-printed carbon electrode modified with graphite nanosheets and zinc oxide nanoparticles. *Microchim Acta* 181:1843–1850
- Liu S, Tian J, Wang L, Luo Y, Lu W, Sun X (2011) Self-assembled graphene platelet-glucose oxidase nanostructures for glucose biosensing. *Biosens Bioelectron* 26:4491–4496
- Li D, Muller B, Gilje S, Kaner RB, Wallace GG (2008) Processable aqueous dispersions of graphene nanosheets. *Nat Nanotechnol* 3:101–105
- Wang F, Gong WC, Wang LL, Chen ZL (2015) Enhanced amperometric response of a glucose oxidase and horseradish peroxidase based bienzyme glucose biosensor modified with a film of polymerized toluidine blue containing reduced graphene oxide. *Microchim Acta* 182:1949–1956
- Kang XH, Wang J, Wu H, Ilhan AA, Liu J, Lin YH (2009) Glucose oxidase-graphene-chitosan modified electrode for direct electrochemistry and glucose sensing. *Biosens Bioelectron* 25:901–907
- Wang CY, Tan XR, Chen SH, Yuan R, Hu FX, Yuan DH, Xiang Y (2012) Highly-sensitive cholesterol biosensor based on platinum-gold hybrid functionalized ZnO nanorods. *Talanta* 94:263–270
- Li YF, Liu ZM, Liu YL, Yang YH, Shen GL, Yu RQ (2006) A mediator-free phenol biosensor based on immobilizing tyrosinase to ZnO nanoparticles. *Anal Biochem* 349:33–40
- Zhang F, Wang X, Ai S, Sun Z, Wan Q, Zhu Z, Xian Y, Jin L, Yamamoto K (2004) Immobilization of uricase on ZnO nanorods for a reagentless uric acid biosensor. *Anal Chim Acta* 519:155–160
- Wang Q, Zheng JB (2010) Electrodeposition of silver nanoparticles on a zinc oxide film: improvement of amperometric sensing sensitivity and stability for hydrogen peroxide determination. *Microchim Acta* 169:361–365
- Ahmad M, Pan C, Gan L, Nawaz ZS, Zhu J (2010) Highly sensitive amperometric cholesterol biosensor based on Pt-Incorporated fullerene-like ZnO nanospheres. *J Phys Chem C* 114:243–250
- Norouzi P, Ganjali H, Larijani B, Ganjali MR, Faridbod F, Zamani HA (2011) A glucose biosensor based on nanographene and ZnO nanoparticles using FFT Continuous cyclic voltammetry. *Int J Electrochem Sci* 6:5189–5199
- Huang JY, Zhao MG, Ye ZZ (2014) Electrospun porous ZnO nanofibers for glucose biosensors. *Adv Mater Res* 950:3–6
- Ali USM, Nur O, Willander M, Danielsson B (2009) Glucose detection with a commercial MOSFET using a ZnO nanowires extended gate. *IEEE Transactions on Nanotechnology* 8:678–683
- Li ZJ, Xie CC, Wang JH, Meng AL (2015) Direct electrochemistry of cholesterol oxidase immobilized on chitosan-graphene and cholesterol sensing. *Sensors Actuators B* 208:505–511
- Meng AL, Shao J, Fan XY, Wang JH (2014) Rapid synthesis of a flower-like ZnO/rGO/Ag micro/nano-composite with enhanced photocatalytic performance by a one-step microwave method. *RSC Adv* 4:60300–60305
- Yang D, Velamakanni A, Bozoklu G, Park S, Stoller M, Piner RD, Stankovich S, Jung I, Field DA, Ventrice CA, Ruoff RS (2009) Chemical analysis of graphene oxide films after heat and chemical treatments by X-ray photoelectron and micro-Raman spectroscopy. *Carbon* 47:145–152
- Liu YG, Feng XM, Shen JM, Zhu JJ (2008) Fabrication of a novel glucose biosensor based on a highly electroactive polystyrene/polyaniline/Au nanocomposite. *J Phys Chem B* 112:9237–9242
- Battaglini F, Bartlett PN, Wang JH (2000) Covalent attachment of osmium complexes to glucose oxidase and the application of the

- resulting modified enzyme in an enzyme switch responsive to glucose. *Anal Chem* 72:502–509
26. Shan D, Zhang J, Xue HG, Ding SN, Cosnier S (2010) Colloidal laponite nanoparticles: extended application in direct electrochemistry of glucose oxidase and reagentless glucose biosensing. *Biosens Bioelectron* 25:1427–1433
 27. Laviron E (1979) General expression of the linear potential sweep voltammogram in the case of diffusionless electrochemical systems. *J Electroanal Chem* 101:19–28
 28. Wu P, Shao Q, Hu YJ, Jin J, Yin YJ, Zhang H (2010) Direct electrochemistry of glucose oxidase assembled on graphene and application to glucose detection. *Electrochim Acta* 55:8606–8614
 29. Xiao XL, Zhou B, Zhu L, Xu LL, Tan L, Tang H (2012) An reagentless glucose biosensor based on direct electrochemistry of glucose oxidase immobilized on poly (methylene blue) doped silica nanocomposites. *Sensors Actuators B Chem* 165:126–132
 30. Zhu L, Xu LL, Tan L, Tan H (2013) Direct electrochemistry of cholesterol oxidase immobilized on gold nanoparticles-decorated multiwalled carbon nanotubes and cholesterol sensing. *Talanta* 106:192–199
 31. Scott DL, Bowden EF (1994) Enzyme-substrate kinetics of adsorbed cytochrome c peroxidase on pyrolytic graphite electrodes. *Anal Chem* 66:1217–1223
 32. Jiang HD, Kim SK (2012) A glucose biosensor based on TiO₂-graphene composite. *Biosens Bioelectron* 38:184–188
 33. Chen XL, Chen JH, Deng CY, Xiao CH, Yang YM, Nie Z (2008) Amperometric glucose biosensor based on boron-doped carbon nanotubes modified electrode. *Talanta* 76:763–767
 34. Oztekin Y, Ramanaviciene A, Yazicigil Z, Solak AO, Ramanavicius A (2011) Direct electron transfer from glucose oxidase immobilized on polyphenanthroline-modified glassy carbon electrode. *Biosens Bioelectron* 26:2541–2546
 35. Du Y, Luo XL, Xu JJ, Chen HY (2007) A simple method to fabricate a chitosan-gold nanoparticles film and its application in glucose biosensor. *Bioelectrochem* 70:342–347